PROJECT ACRONYM

**CUPIDO**

PROJECT TITLE

**Cardio Ultraefficient nanoParticles for Inhalation of Drug prOducts**

# Deliverable 4.5

# Extended model, describing relationship between $^{Fe}$CaPs and deposition site when exposed to an external magnetic field

| | | | |
|---|---|---|---|
| CALL ID | | | H2020-NMBP-2016-2017 |
| GA No. | | | 720834 |
| MAIN CONTACT | | | **Kristian Valen-Sendstad**<br>Email: kvs@simula.no |
| NATURE | Report (R) | DISSEMINATION LEVEL | PU |
| DUE DATE | 31/07/2019 | ACTUAL DELIVERY DATE | 01/08/2019 |
| AUTHOR(S) | | | Alexandra Diem, Kristian Valen-Sendstad |

# Table of Revisions

| REVISION NO. | DATE | WORK PERFORMED | CONTRIBUTOR(S) |
|---|---|---|---|
| 1 | 10/06/2019 | Document preparation | Alexandra Diem, Kristian Valen-Sendstad |
| 2 | 10/06/2019 | Revision | Daniele Catalucci |
| 3 | 29/07/2019 | Revision | IPR Team |
| 4 | 30/07/2019 | Formatting | Paulina Piotrowicz |

# Table of Contents

1. Executive summary ..... 4
2. Cooperation between participants ..... 4
3. Simulations of $^{Fe}$CaPs in the human heart when exposed to an external magnetic field ..... 5
3.1. A novel particle tracking-based method to simulate drug delivery ..... 5
3.1.1. Introduction ..... 5
3.1.2. Methods ..... 5
3.1.3. Results ..... 7
4. Conclusions ..... 11

# Index of Figures and Tables

**Figure 1:** Perfusion pressure in units of kPa (a) and velocity magnitude in units of mm/s (b) in the three compartments (from left to right: large arterioles, small arterioles, capillaries; small arterioles and capillaries share the same colour bar). Pressure values range between 22-25 mmHg, which agree with the simulation results presented in Michler et al. (2013), whilst our simulation reaches a faster peak velocity magnitude of 0.6 mm/s compared to the results by Michler et al. (2013). The large arterioles compartment (left) shows the largest gradients in both pressure and velocity. The capillary compartment shows very small pressure gradients of 1 mmHg, with a corresponding peak velocity of 0.1 mm/s. ..... 7
**Figure 2:** Nanoparticle distribution in the left ventricle geometry over three cardiac cycles at $t$ = 1.0, 2.0, 3.0 s (left to right). Values are shown as a fraction of the maximum concentration. ..... 8
**Figure 3:** Nanoparticle distribution in the left ventricle geometry over three cardiac cycles at time intervals of 0.5 s (left to right; top to bottom). Only elements containing a concentration larger than 0.1 (10%) of the maximum concentration) are shown. ..... 8
**Figure 4:** Total concentration of NP in the left ventricle over three cardiac cycles. ..... 9
**Figure 5:** Difference Δc in total concentration of NP between CaPs and $^{Fe}$CaPs. The data was fit to a quadratic function with $f(x) = 0.61280339\ x^2 - 0.32995026x + 0.14529408$. ..... 9

# 1. Executive summary

This deliverable extends the work described in deliverables D4.1 and D4.2 and focusses on modelling $^{Fe}$CaPs in the human heart. The model is based on our novel particle-based tracking method using a splitting method on the conventional reaction-advection-diffusion equation that is currently under review for journal publication. We used this model to compare NP distributions in the left ventricle between CaP and $^{Fe}$CaP, which demonstrate that distribution patterns are influenced by the presence of magnetic forces as calculated in deliverable D4.1.

**Key deliverable achievements**:

1. Development of a novel particle-based tracking model based on using a splitting method on the conventional reaction-advection-diffusion equation.
2. Comparison of NP distributions between CaP and $^{Fe}$CaP.
3. Journal publication currently under review.

# 2. Cooperation between participants

SIM collaborated with CNR-IEIIT for the achievement of the objectives for D4.5. Specifically, CNR-IEIIT carried out initial simulations to evaluate the feasibility of using different types of magnets to guide nanoparticles (D4.1). All parameters used in the simulations for this deliverable are based on data obtained for D4.1.

# 3. Simulations of $^{Fe}$CaPs in the human heart when exposed to an external magnetic field

## 3.1. A novel particle tracking-based method to simulate drug delivery

### 3.1.1. Introduction

Heart tissue is perfused by thousands of very small arteries and capillaries branching off the coronary arteries. Obtaining truthful representations of the exact geometries of the perfusion circulation using state-of-the-art imaging techniques is virtually impossible. Instead, as detailed in previous deliverables, we regard heart tissue as a porous material and use continuum models to obtain approximate solutions of perfusion pressure and flow velocities, following the work of Michler et al. (2013). Here, perfused heart tissue is modelled as a superposition of three porous materials that represent perfusion at the artery, arteriole, and capillary level. These models are highly nonlinear and thus require fine meshes and small-time steps, leading to large computational costs. Thus, in mechanics modelling, these models are usually simulated for one heartbeat (~ 1 s) and it is appropriate to extrapolate these results to multiple heart beats. However, when one is interested in modelling the distribution of nanoparticle-based therapeutic compounds, this extrapolation from one heartbeat to a series of over 30 heartbeats is no longer appropriate. Experimental effects are expected to take place over the course of approximately 30 minutes (Miragoli et al. 2018) and thus, in order to be able to predict efficacy and efficiency of administered compounds and their delivery vehicles and dosages, it is necessary to simulate the complete experimental duration, requiring the use of efficient numerical methods.

In this deliverable we present a method based on Lagrangian particle tracking that provides a significant improvement in both computational cost and accuracy of the results, compared to conventionally used methods (Diem and Valen-Sendstad 2019). The method is based on the assumption that blood flow velocities in the large and small arterioles results in large Peclet numbers, which renders the use of advection-diffusion kinetics inadequate. Instead, we assume that the location of nanoparticles is solely influenced by advection, taking into account the directionality of cardiac muscle fibers. Perfusion in capillaries on the other hand is assumed to be isotropic and thus represented by diffusion, using a large diffusion coefficient based on capillary flow velocities. To obtain perfusion velocities in the large arterioles, small arterioles, and capillaries, perfusion is represented by a three-compartment porous media continuum model based on Darcy's law as previously done by other groups (Chapelle et al. 2010, Michler et al. 2013), while nanoparticle delivery is approximated by splitting advection and diffusion kinetics across compartments. We demonstrate the efficiency of our method by simulating perfusion to the left ventricle over multiple cardiac cycles using a conventional laptop, instead of having to rely on the use of a high-performance computing cluster.

### 3.1.2. Methods

Perfusion through the heart tissue is modelled using a multi-compartment porous media model that has previously been described in detail in deliverable D4.2

$$-\nabla \cdot (\mathbf{K}_i \cdot \nabla p_i) + \sum_{k=1}^{N} \beta_{i,k}(p_i - p_k) = s_i$$

Where $\boldsymbol{K}_i$ are permeability tensors of the $N$ different compartments, $p_i$ is pressure and $\beta_{i,k}$ are compartment exchange coefficients. To model perfusion to the heart, we use $N = 3$, to represent arteries, arterioles and capillaries. Blood flow velocity $\boldsymbol{w}_i$ in each compartment can then be recovered using Darcy's law

$$\mathbf{w}_i = -\mathbf{K}_i \nabla p_i$$

Nanoparticle distribution is modelled in the same fashion as the distribution of, for example, an MRI contrast agent (Cookson et al. 2014), using standard, transient advection-diffusion kinetics for each compartment *I*

$$\frac{\partial c_i}{\partial t} = \nabla \cdot (D_i \nabla c_i) - \mathbf{w}_i \cdot \nabla c_i + \sum_{k=1}^{3} \gamma_{i,k} c_i + s_i \qquad \text{in } \Omega.$$

with $c_i$ nanoparticle concentration, $D_i$ diffusion coefficient, $\boldsymbol{w}_i$ advection velocity, $\gamma_{i,k}$ exchange coefficients between compartments *i* and *k*, and $s_i$ source/sink terms.

Deposition of nanoparticles into myocardial tissue is assumed to strongly rely on margination (Carboni et al. 2014), which allows for endocytosis of nanoparticles into myocardial cells. As margination occurs at the blood vessel wall, this process relies on small fluid velocities such that nanoparticles are able to move across fluid streamlines. The reliance on endocytosis after margination at low shear rates that allow for sufficient adhesion time of nanoparticles at the blood vessel wall has been shown in a number of studies (Toy et al. 2011, Namdee et al. 2013, Carboni et al. 2014). Thus, it is most likely that nanoparticle deposition occurs primarily within the capillary compartment. The non-linear advection-diffusion equation is time consuming to solve and is well known to be unstable at high Peclet numbers, where the effects of advection dominate over the effects of diffusion

$$\mathrm{Pe} = \frac{||\mathbf{w}||h}{2D}$$

for velocity norm $||\boldsymbol{w}||$ and mesh element size *h*. To overcome this problem, we introduce the following splitting method: We assume that advection dominates strongly in artery and arteriole compartments, such that diffusion can be neglected. Thus, we can approximate the position $\boldsymbol{x}$ of any particle advected by the fluid evolves according to a simple first order transient model

$$\frac{\partial \mathbf{x}}{\partial t} = \mathbf{w}$$

To efficiently track nanoparticles through the myocardium we model a *bolus* as a collection of nanoparticles using Lagrangian particle tracking in the artery and arteriole bed (compartments 1 and 2). Furthermore, while blood flow in perfusion arterioles is generally considered to follow muscle fiber directions, we assume that capillary flow within the myocardium is isotropic. Therefore, we can approximate the distribution of nanoparticles in the capillary compartment by a sufficiently large diffusion coefficient that represents the velocity of capillary flow. The combined nanoparticle tracking model equation thus reads

$$\frac{\partial \mathbf{x}_i}{\partial t} = \mathbf{w}_i \quad i = 1, 2 \qquad \text{in } \Omega$$

$$\frac{\partial c_3}{\partial t} = \nabla \cdot (D_3 \nabla c_3) + \gamma_{2,3} c_2 + s_3 \qquad \text{in } \Omega.$$

To add magnetic force to the model the second equation is extended to

$$\frac{\partial c_3}{\partial t} = \nabla \cdot (D_3 \nabla c_3) - \nabla \cdot (\xi^{-1} \mathbf{F} c) + \gamma_{2,3} c_2 + s_3 \qquad \text{in } \Omega.$$

With magnetic force F, balanced by nanoparticle drag force ξ. Magnetic forces are not added to the first equation as it was concluded in D4.1 that no externally placed magnet would be able to overcome drag forces at the blood vessel center line.

The model is implemented in Python 3.5.2 using the finite element framework FEniCS (Alnæs et al. 2015). In FEniCS the implementation of the variational form is very similar to the mathematical formulation, allowing for a simple conversion of equations to code. Coupled equations containing multiple unknowns like the multi-compartment formulation of Darcy's law are implemented using a mixed finite element.

### 3.1.3.Results

**Table 1:** Simulation parameters for the left ventricle simulation.

| Parameter | Unit | Value | Physical meaning |
|---|---|---|---|
| $K_1$ | $mm^2\ kPa^{-1}\ s^{-1}$ | 1 | Permeability |
| $K_2$ | $mm^2\ kPa^{-1}\ s^{-1}$ | 10 | Permeability |
| $K_3$ | $mm^2\ kPa^{-1}\ s^{-1}$ | 20 | Permeability |
| $\Phi_1$ | 1 | 0.021 | Porosity |
| $\Phi_2$ | 1 | 0.029 | Porosity |
| $\Phi_3$ | 1 | 0.061 | Porosity |
| $\beta_{1,2}$ | $Pa^{-1}\ s^{-1}$ | 0.02 | Compartment exchange coefficient for pressure |
| $\beta_{2,3}$ | $Pa^{-1}\ s^{-1}$ | 0.05 | Compartment exchange coefficient for pressure |
| $\gamma_{1,2}$, $\gamma_{2,3}$ | 1 | 0.5 | Compartment exchange coefficients for NP |
| $D_3$ | $mm^2$ | 1.0 | Effective diffusion coefficient that mimicing capillary flow velocity |
| $\Delta t$ | s | $1 \times 10^{-4}$ | Time step |
| $\xi$ | N | $1.7 \times 10^{-15}$ | NP drag force |
| $\boldsymbol{F}$ | N | $1.2 \times 10^{-13}$ | Magnetic field force |

Following successful initial tests of the particle tracking method on a 2D unit square mesh (Diem and Valen-Sendstad 2019), we applied the same method to modelling perfusion of the left ventricle. The simulation parameters are listed in **Table 1**, where parameters relating to the pressure equations are taken from Michler et al. 2013. In the literature, the average capillary flow velocity has been reported as 1 mm/s (Ivanov et al. 1981) and thus $D_3$ has been chosen as 1 $mm^2$ accordingly, while $\gamma$ has been chosen to provide nanoparticle distribution within a reasonable time frame (~ one cardiac cycle).

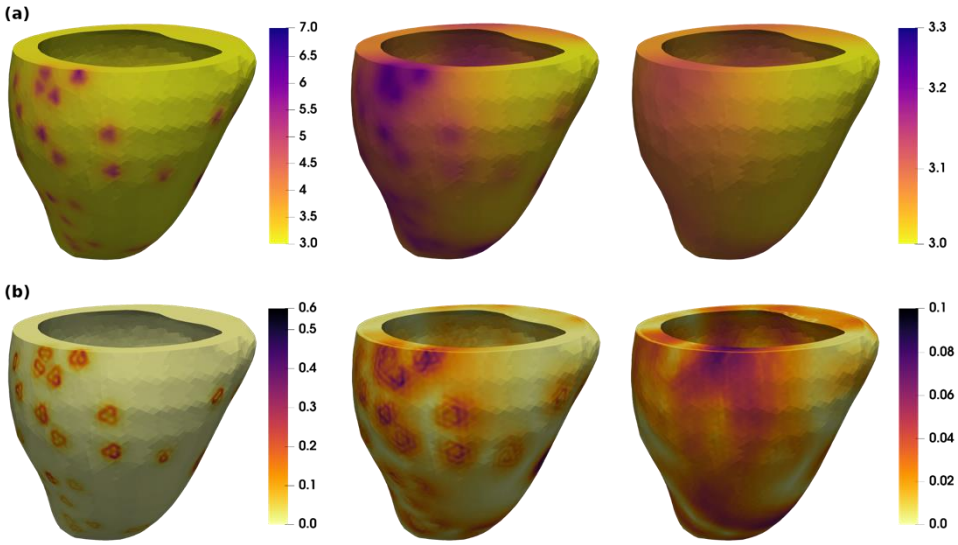


**Figure 1:** Perfusion pressure in units of kPa (a) and velocity magnitude in units of mm/s (b) in the three compartments (from left to right: large arterioles, small arterioles, capillaries; small arterioles and capillaries share the same colour bar). Pressure values range between 22-25 mmHg, which agree with the simulation results presented in Michler et al. (2013), whilst our simulation reaches a faster peak velocity magnitude of 0.6 mm/s compared to the results by Michler et al. (2013). The large arterioles compartment (left) shows the largest gradients in both pressure and velocity. The capillary compartment shows very small pressure gradients of 1 mmHg, with a corresponding peak velocity of 0.1 mm/s.

The results of the perfusion model are shown **Figure 1**. Pressure values in the left ventricle range between 22-55 mmHg, which agree with the simulation results presented in Michler et al. 2013, whilst our simulation reaches a faster peak velocity magnitude of 0.6 mm/s compared to the results by Michler et al. (2013). The differences can most likely be attributed to different distributions of the blood flow entry points to the myocardium. The large arterioles compartment shows the largest gradients in both pressure and velocity. The capillary compartment shows very small pressure gradients of 1 mmHg, with a corresponding peak velocity of 0.1 mm/s. These results indicated that it is appropriate to disregard velocities within the capillary compartment and instead use a diffusion coefficient that matches capillary flow conditions. The results of the nanoparticle deposition simulations show that after one cardiac cycle 55% of the myocardial tissue is perfused. Complete perfusion is reached shortly after the second cardiac cycle.

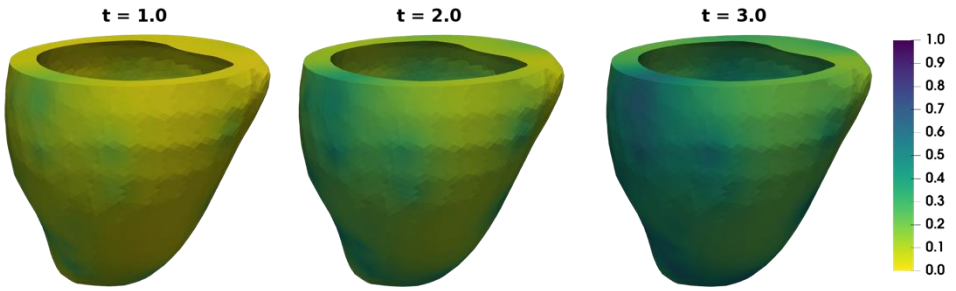


**Figure 2:** Nanoparticle distribution in the left ventricle geometry over three cardiac cycles at *t* = 1.0, 2.0, 3.0 s (left to right). Values are shown as a fraction of the maximum concentration.

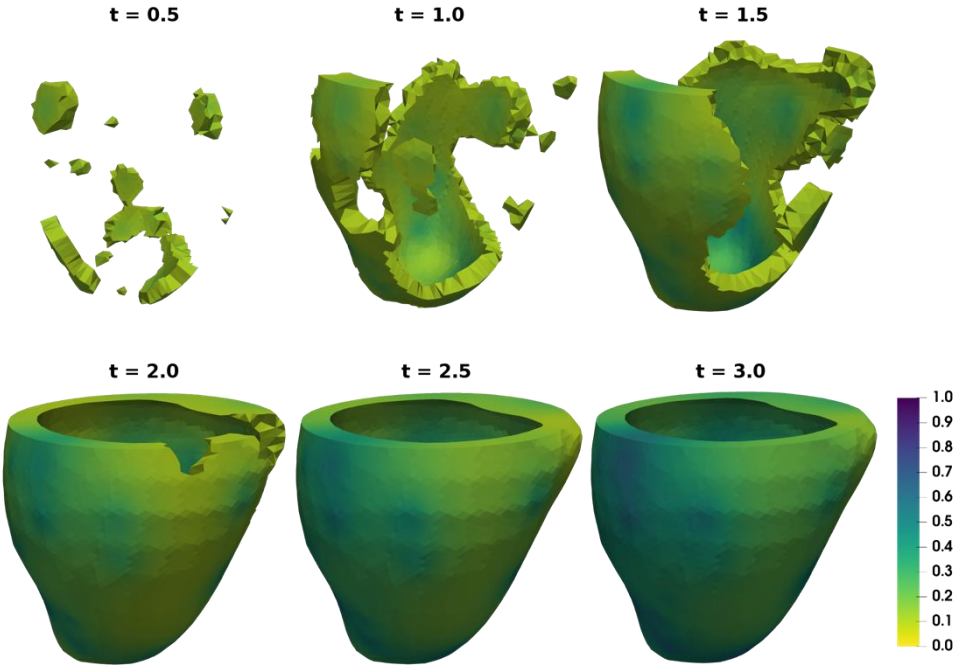


**Figure 3:** Nanoparticle distribution in the left ventricle geometry over three cardiac cycles at time intervals of 0.5 s (left to right; top to bottom). Only elements containing a concentration larger than 0.1 (10%) of the maximum concentration) are shown.

The above results on perfusion pressure and velocity in the left ventricle were used to drive the NP tracking model. **Figure 2** and **Figure 3** show the distribution of nanoparticles within the myocardium, using the pressure and velocity data from **Figure 1**. **Figure 2** shows the distribution of nanoparticles in the left ventricle over three cardiac cycles at *t* = 1.0, 2.0, 3.0 s (left to right). In order to study the pattern and time frame of perfusion and the distribution of nanoparticles, **Figure 3** shows the same distribution at intervals of 0.5 s. Additionally, only elements with a *c* > 0.1 are shown to illustrate the process of perfusion with NP. These results show that after

one cardiac cycle 55% of the myocardial tissue are perfused. Complete perfusion is reached shortly after the second cardiac cycle.

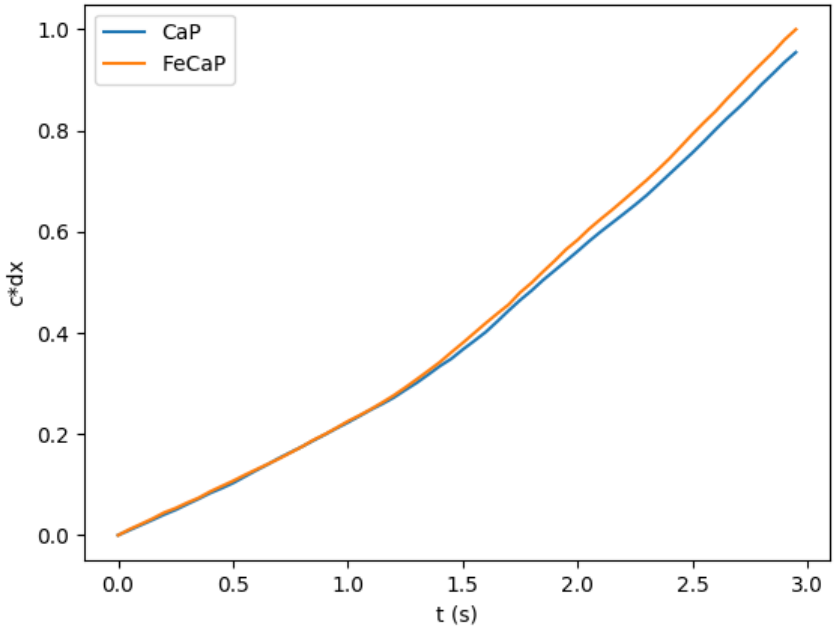


**Figure 4:** Total concentration of NP in the left ventricle over three cardiac cycles.

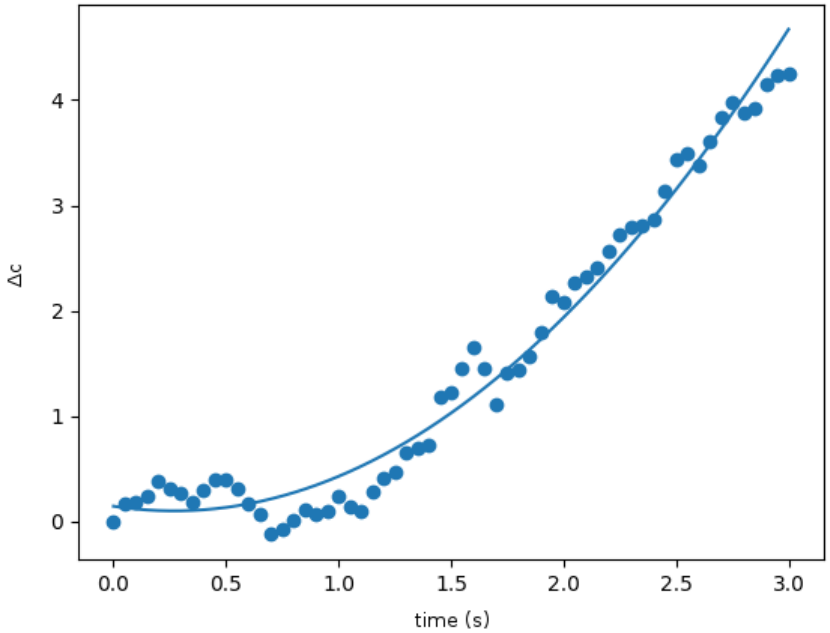


**Figure 5:** Difference Δc in total concentration of NP between CaPs and $^{Fe}$CaPs. The data was fit to a quadratic function with *f(x) = 0.61280339 x$^2$ - 0.32995026x + 0.14529408.*

**Figure 4** shows the difference in total concentration of NP within the left ventricle between CaP and $^{Fe}$CaP. After three cardiac cycles the total difference in concentration was 4.44%. With CaPs, maximum perfusion of the left ventricle was achieved after 1.82 s, while it was reached after 1.35 s, indicating that the use of $^{Fe}$CaPs has an overall positive effect on the distribution of NP.

**Figure 5** shows the difference in total concentration of NP between CaPs and $^{Fe}$CaPs data. A curve fit shows that the function

$$f(x) = 0.61280339\,x^2 - 0.32995026x + 0.14529408$$

best describes the data, indicating that longer, experimentally relevant time frames of around 30 minutes will lead to much larger differences in deposition between CaPs and $^{Fe}$CaPs, depending on the protocol of administration. These results demonstrate a potential benefit of the use of magnets on the patterns of NP distribution between $^{Fe}$CaPs and CaPs.

One limitation of this study is, however, that the model cannot account for the exact location of the magnet, such that the same magnetic force is applied on the entire geometry. We have additionally intensively tested the use of a poroelastic model that combines perfusion with cardiac contraction. Due to the numerical difficulty in solving such a coupled model, this work is ongoing, but expected to deliver more realistic results of NP distribution. Specifically, the poroelastic model cannot yet account for the large strains the heart undergoes during contraction.

# 4. Conclusions

The model presented here is based on our novel particle-based tracking method using a splitting method on the conventional reaction-advection-diffusion equation that is currently under review for journal publication. We used this model to compare NP distributions in the left ventricle between CaP and $^{Fe}$CaP, which demonstrate that distribution patterns are influenced by the presence of magnetic forces as calculated in deliverable D4.1. The model shows that the difference in distribution grows with a quadratic function over time, and full perfusion is much faster using $^{Fe}$CaP, compared to CaP. These results indicate that the use of magnetic forces to manipulate NP distribution and deposition is viable.

## References


Alnæs MS, Blechta J, Hake J, Johansson A, Kehlet B, et al. (2015) The FEniCS Project Version 1.5. Archive of Numerical Software 3.

Carboni E, Tschudi K, Nam J, Lu X, and Ma AWK (2014) Particle Margination and Its Implications on Intravenous Anticancer Drug Delivery. AAPS PharmSciTech 15: 762-771.

Cookson AN, Lee J, Michler C, Chabiniok R, Hyde E, et al. (2014) A spatially-distributed computational model to quantify behaviour of contrast agents in MR perfusion imaging. Medical Image Analysis 18: 1200-1216.

Chapelle D, Gerbeau JF, Sainte-Marie J, and Vignon-Clementel IE (2010) A poroelastic model valid in large strains with applications to perfusion in cardiac modelling. Computational Mechanics 46: 91-101.

Diem AK, and Valen-Sendstad K (2019) In-silico timelapse of perfusion: A novel particle tracking-based method to simulate drug delivery. Biophysical Journal, under review.

Ivanov KP, Kalinina MK, and Levkovich YI (1981) Flow Velocity in Capillaries of Brain and Muscles: Physiological Significance. Microvascular Research 22: 143-155.

Michler C, Cookson AN, Chainiok R, Hyde E, Lee J, et al. (2013) A computationally efficient framework for the simulation of cardiac perfusion using a multi-compartment Darcy porous-media flow model. International Journal for Numerical Methods in Biomedical Engineering 29: 217-232.

Miragoli M, Ceriotti P, Iafisco M, Vacchiano M, Salvarani N, et al. (2018) Inhalation of peptide-loaded nanoparticles improves heart failure. Science Translational Medicine 10.

Namdee K, Thompson AJ, Charoenphol P, and Eniola-Adefeso (2013) Margination Propensity of Vascular-Targeted Spheres from Blood Flow in a Microfluidic Model of Human Microvessels. Langmuir 29: 2530-2535.

Toy R, Haden E, Shoup C, Baskaran H, and Karathanasis E (2011) The effects of particle size, density and shape on margination of nanoparticles in microcirculation. Nanotechnology 22: 115101.